

**Supporting Information**

**A thermochromic macrocyclic materials exhibiting slow relaxation of the magnetization: support for magnetic response and visualization applications**

Han Yan <sup>a</sup>, Jia-Ling Wang <sup>a</sup>, Hao Wang <sup>a</sup>, Hai-Quan Tian <sup>b</sup> and Wen-Bin Sun <sup>\*a</sup>

<sup>a</sup> Key Laboratory of Functional Inorganic Material Chemistry Ministry of Education, School of Chemistry and Material Science Heilongjiang University, 74 Xuefu Road, Harbin 150080, P. R. China.

E-mail: [wenbinsun@126.com](mailto:wenbinsun@126.com)

<sup>b</sup> Shandong Provincial Key Laboratory of Chemical Energy Storage and Novel Cell Technology, School of Chemistry and Chemical Engineering, Liaocheng University, Liaocheng 252059, P. R. China.

**Table S1** Crystallographic data for complexes **1**, **2**, **3-Dy** and **3-Dy\***.

	<b>1</b>	<b>2</b>	<b>3-Dy</b>	<b>3-Dy*</b>
formula	C <sub>16</sub> H <sub>27</sub> Cl <sub>3</sub> DyN <sub>5</sub> O <sub>5</sub>	C <sub>28</sub> H <sub>29</sub> Cl <sub>5</sub> DyN <sub>7</sub> O <sub>7</sub>	C <sub>36</sub> H <sub>58</sub> Cl <sub>4</sub> Dy <sub>2</sub> N <sub>10</sub> O <sub>12</sub>	C <sub>36</sub> H <sub>58</sub> Cl <sub>4</sub> Dy <sub>2</sub> N <sub>10</sub> O <sub>12</sub>
FW (g.mol <sup>-1</sup> )	638.27	915.33	1289.72	1289.72
Crystal system	triclinic	monoclinic	monoclinic	monoclinic
Space group	P-1	P2 <sub>1</sub> /n	C2/c	C2/c
Temperature (K)	213(2)	293(2)	293.15	293(2)
a (Å)	8.7379(3)	15.4334(7)	18.4652(16)	18.5354(12)
b (Å)	11.3821(4)	11.5838(3)	21.993(2)	22.0457(19)
c (Å)	11.4772(4)	20.6732(10)	11.7138(11)	11.7708(8)
α (°)	92.571(2)	90	90	90
β (°)	99.667(3)	111.779(5)	94.456(8)	95.201(7)
γ (°)	90.403(3)	90	90	90
V (Å <sup>3</sup> )	1124.01(7)	3432.1(3)	4742.7(7)	4790.1(6)
ρcacd (Mg.m <sup>-3</sup> )	1.886	1.771	1.806	1.788
μ (mm <sup>-1</sup> )	21.399	15.708	3.420	3.386
F (000)	630.0	1812.0	2560.0	2560
Collected reflections	10919	36464	13097	15735
Independent relections	3975	6115	4149	4207
Rint	0.0580	0.1371	0.0847	0.0725
R1 [I > 2σ(I)]	0.0345	0.0611	0.1028	0.0707
wR <sub>2</sub> (all data)	0.0875	0.1866	0.2344	0.1558
GOF	1.051	1.071	1.182	1.116
CCDC number	2344863	2344862	2344861	

**Table S2** Selected bond lengths (Å) and angles (°) for complexes **1** and **2**.

	<b>1</b>	<b>2</b>	
Dy-Cl1	2.7065(10)	Dy-Cl	2.7736(19)
Dy-Cl2	2.7104(10)	Dy-O1	2.259(5)
Dy-O	2.432(3)	Dy-O4	2.341(5)

Dy-N1	2.459(3)	Dy-N1	2.474(5)
Dy1-N2	2.455(3)	Dy-N2	2.539(6)
Dy1-N3	2.508(3)	Dy-N4	2.470(6)
Dy1-N4	2.481(3)	Dy-N6	2.461(6)
Dy1-N5	2.436(3)	Dy-N7	2.522(6)
Cl1-Dy-Cl2	146.78(3)	O1-Dy-Cl	145.29(16)
O1-Dy-Cl1	143.66(8)	O1-Dy-O4	78.0(2)
O1-Dy-Cl2	69.54(8)	O4-Dy-Cl	136.59(15)

**Table S3** Selected bond lengths ( $\text{\AA}$ ) and angles ( $^\circ$ ) for complexes **3-Dy** and **3-Dy\***.

3-Dy		3-Dy*	
Dy1-Cl1	2.678(5)	Dy*1-Cl1	2.690(3)
Dy1-O1	2.192(17)	Dy*1-O1	2.214(9)
Dy1-O1'	2.245(15)	Dy*1-O1'	2.222(9)
Dy1-N1	2.452(17)	Dy*1-N1	2.427(12)
Dy1-N2	2.408(18)	Dy*1-N2	2.455(10)
Dy1-N3	2.471(14)	Dy*1-N3	2.442(11)
Dy1-N4	2.443(18)	Dy*1-N4	2.434(10)
Dy1-N5	2.394(18)	Dy*1-N5	2.443(10)
O1-O2	1.43(3)	O1-O2	1.431(19)
O1-Dy1-Cl	158.3(4)	O1-Dy*1-Cl1	157.9(3)
O2-Dy1-Cl	164.2(5)	O2-Dy*1-Cl1	164.4(3)
O1-Dy1-O2	37.5(8)	O1-Dy*1-O2	37.6(8)
Dy1-O1-Dy2	142.4(8)	Dy*1-O1-Dy2	142.4(5)

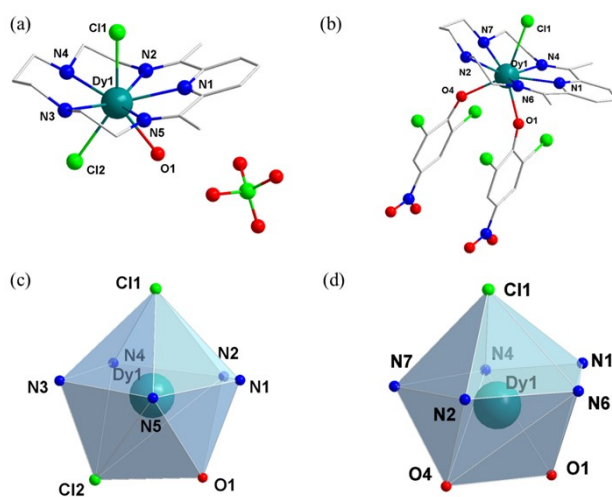


**Fig. S1** Structure of complexes **1** (a) and **2** (b). Coordination polyhedra for complexes **1** (c) and **2** (d).

**Table S4** Continuous Shape Measures (CShMs) of the coordination geometry for Dy<sup>III</sup> ion in complexes **1-3**. (CShMs

values calculated with the Shape program). The CShMs values indicated the proximity to the ideal polyhedron, thus, CShMs = 0 corresponds to the non-distorted polyhedron. The three closer ideal geometries to the real complexes are listed and below are the symmetry and description for each polyhedron.

	CShMs	Polyhedron	
<b>1</b>	1.788	TDD-8	$D_{2d}$ Triangular dodecahedron
	2.733	BTPR-8	$C_{2v}$ Biaugmented trigonal prism
	3.928	JBTPR-8	$C_{2v}$ Biaugmented trigonal prism J50
<b>2</b>	2.101	TDD-8	$D_{2d}$ Triangular dodecahedron
	2.720	BTPR-8	$C_{2v}$ Biaugmented trigonal prism
	3.695	JBTPR-8	$C_{2v}$ Biaugmented trigonal prism J50
<b>3</b>	4.898	TDD-8	$D_{2d}$ Triangular dodecahedron
	6.474	BTPR-8	$C_{2v}$ Biaugmented trigonal prism
	7.055	JBTPR-8	$C_{2v}$ Biaugmented trigonal prism J50

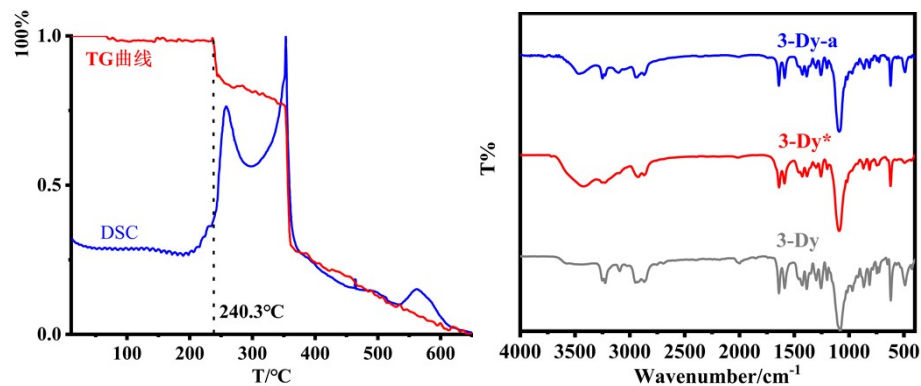


**Fig. S2** TG (red line) and DSC (blue line) curve of **3-Dy** in 12-600 °C (left). Infrared spectra for **3-Dy**, **3-Dy\***, **3-Dy-a** (after heating exposure to air for 3 weeks) in the coloration process (right).

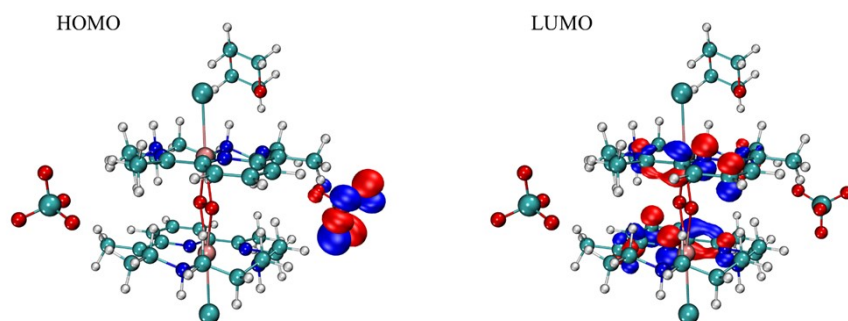


**Fig. S3** HOMO and LUMO energy levels for **3**.

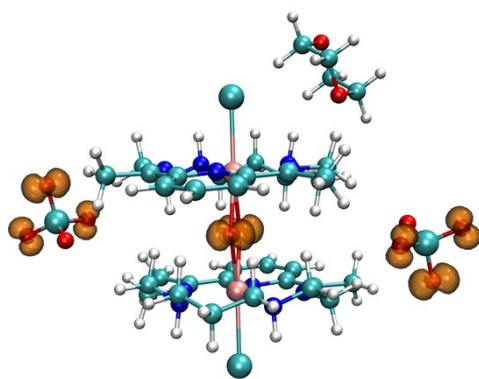


**Fig. S4** Spin population analysis for complex **3**.

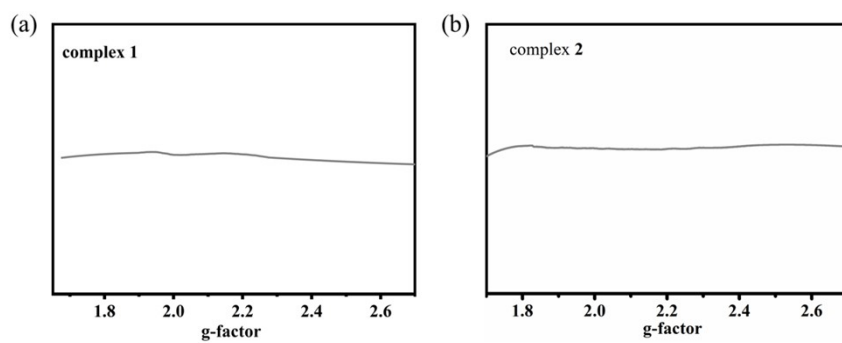


**Fig. S5** EPR spectra of **1** (a), **2** (b) in the solid state after heating.

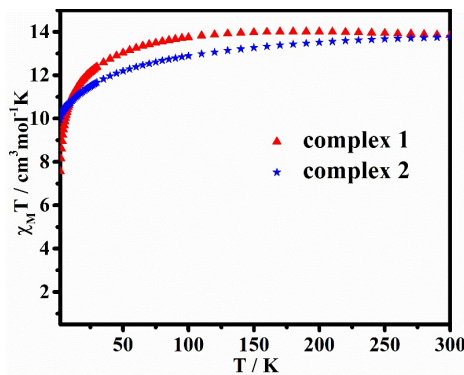


**Fig. S6** Temperature dependence of the magnetic susceptibility  $\chi_M T$  at 1000 Oe for complexes **1** and **2**.

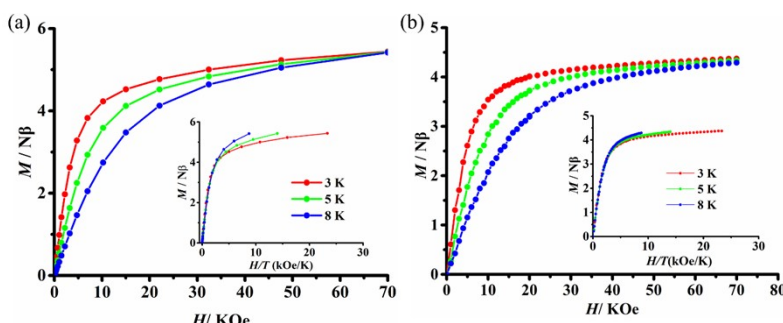


**Fig. S7** Field dependences of magnetization in the field range 0–70 kOe and temperature range 3–8 K for complexes **1** (a) and **2** (b).

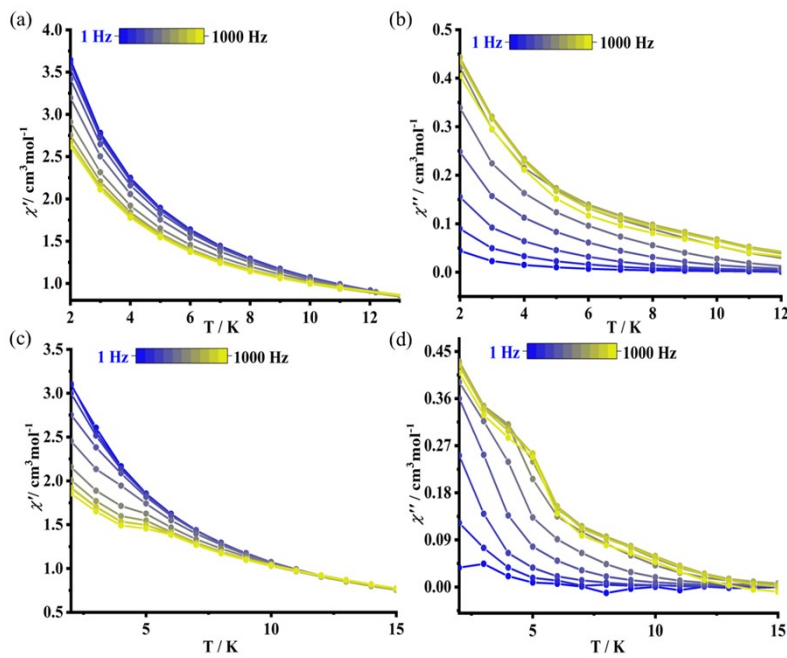


**Fig. S8** Temperature dependence of the in-phase ( $\chi'$ ) ac susceptibility (a) and out-of-phase ( $\chi''$ ) ac susceptibility (b) in the temperature range 2-12 K of complex **1** under 0 Oe. Temperature dependence of the in-phase ( $\chi'$ ) ac susceptibility (c) and out-of-phase ( $\chi''$ ) ac susceptibility (d) in the temperature range 2-15 K of complex **1** under 1500 Oe.

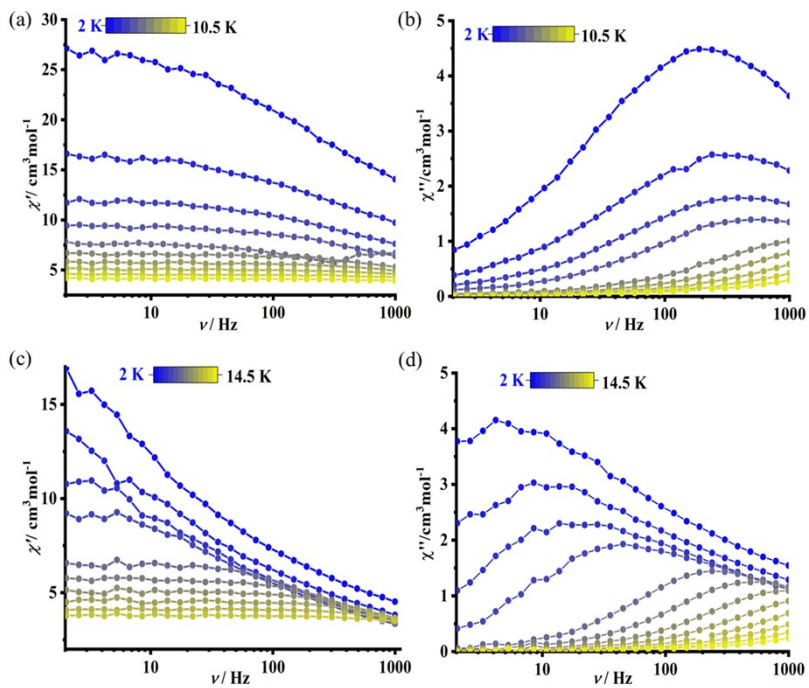


**Fig. S9** Frequency dependence of the in-phase ( $\chi'$ ) ac susceptibility (a) and the out-of-phase ( $\chi''$ ) ac susceptibility (b) in the temperature range 2-10.5 K of **2** under 0 Oe. Frequency dependence of the in-phase ( $\chi'$ ) ac susceptibility (c) and out-of-phase ( $\chi''$ ) ac susceptibility (d) in the temperature range 2-14.5 K of complex **2** under 1000 Oe.

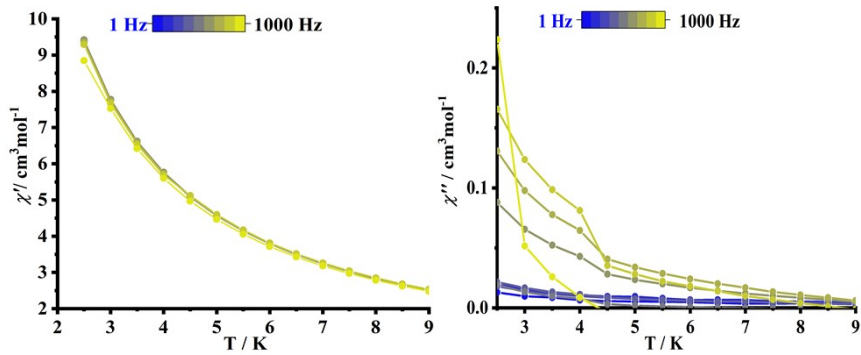


**Fig. S10** Temperature dependence of the in-phase ( $\chi'$ ) ac susceptibility (left) and the out-of-phase ( $\chi''$ ) ac susceptibility (right) in the temperature range 2.5–9 K of **3-Dy** under 0 Oe.

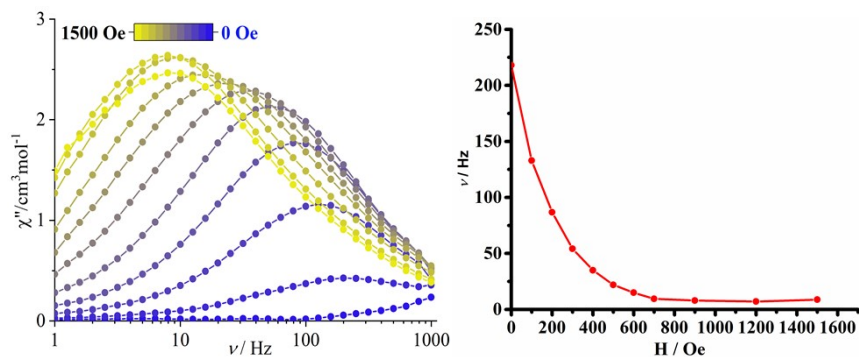


**Fig. S11** Plot of the frequency dependence of the out-of-phase ( $\chi''$ ) ac susceptibility component under indicated dc field at 3 K for **3-Dy** (left). Plot of  $1/\tau$  vs.  $H$  for **3-Dy** under different dc fields at 3 K (right), the solid line is guide for eyes.

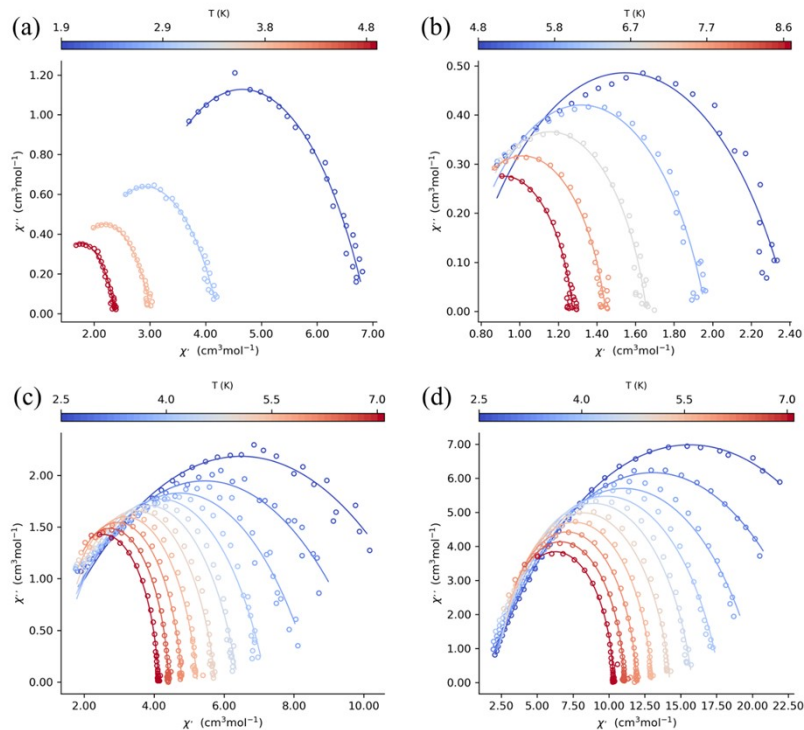


**Fig. S12** Cole-Cole plots for **2** under 0 Oe (a) and 1000 Oe (b). Cole-Cole plots for **3-Dy** (c) and **3-Dy\*** (d) under 1200 Oe. The solid lines are the best fit for the generalized Debye model.

**Table S5.** Best fitted parameters ( $\chi_T$ ,  $\chi_S$ ,  $\tau$  and  $\alpha$ ) with the extended Debye model for complex **2** at 0 Oe in the temperature range 1.9-4.8 K.

T / K	$\chi_S / \text{cm}^3 \text{ mol}^{-1}$	$\chi_T / \text{cm}^3 \text{ mol}^{-1}$	$\tau/\text{s}$	$\alpha$
1.9	2.41334	6.90768	0.00074	0.40782
2.9	1.62330	4.22096	0.00047	0.41834
3.8	1.35562	3.02534	0.00039	0.37031
4.8	1.15479	2.37991	0.00029	0.33339

**Table S6.** Best fitted parameters ( $\chi_T$ ,  $\chi_S$ ,  $\tau$  and  $\alpha$ ) with the extended Debye model for complex **2** at 1000 Oe in the temperature range 4.8-8.6 K.

T / K	$\chi_S / \text{cm}^3 \text{ mol}^{-1}$	$\chi_T / \text{cm}^3 \text{ mol}^{-1}$	$\tau/\text{s}$	$\alpha$
4.8	0.69354	2.39632	0.00240	0.33991
5.7	0.67393	1.96474	0.00113	0.26517
6.7	0.65801	1.65696	0.00058	0.19543
7.7	0.58629	1.44511	0.00030	0.19098
8.6	0.56281	1.27589	0.00017	0.16285

**Table S7.** Best fitted parameters ( $\chi_T$ ,  $\chi_S$ ,  $\tau$  and  $\alpha$ ) with the extended Debye model for complex **3-Dy** at 1200 Oe in the temperature range 2.5-7 K.

T / K	$\chi_S / \text{cm}^3 \text{ mol}^{-1}$	$\chi_T / \text{cm}^3 \text{ mol}^{-1}$	$\tau/\text{s}$	$\alpha$
2.5	1.39560	29.86939	0.04330	0.41950
3.0	1.40983	24.68399	0.02045	0.37975
3.5	1.63150	20.45429	0.00894	0.30641
4.0	1.86695	17.77609	0.00436	0.23267
4.5	2.06496	15.81021	0.00230	0.16799
5.0	2.15188	14.24521	0.00129	0.12203
5.5	2.19636	12.99291	0.00077	0.08665
6.0	2.21196	11.92472	0.00049	0.05917
6.5	2.19863	11.06543	0.00032	0.04439
7.0	2.22403	10.30955	0.00022	0.03218

**Table S8.** Best fitted parameters ( $\chi_T$ ,  $\chi_S$ ,  $\tau$  and  $\alpha$ ) with the extended Debye model for complex **3-Dy\*** at 1200 Oe in the temperature range 2.5-7 K.

T / K	$\chi_s / \text{cm}^3 \text{ mol}^{-1}$	$\chi_T / \text{cm}^3 \text{ mol}^{-1}$	$\tau/\text{s}$	$\alpha$
2.5	0.60109	12.37717	0.00968	0.54786
3.0	0.64208	10.25542	0.00541	0.51016
3.5	0.88848	8.56849	0.00318	0.43425
4.0	1.16754	7.19940	0.00191	0.32422
4.5	1.21407	6.39964	0.00123	0.25762
5.0	1.22301	5.75390	0.00080	0.19492
5.5	1.14080	5.23607	0.00052	0.15616
6.0	1.11194	4.79474	0.00035	0.11105
6.5	1.06478	4.42118	0.00025	0.07680
7.0	0.97395	4.11916	0.00017	0.06131

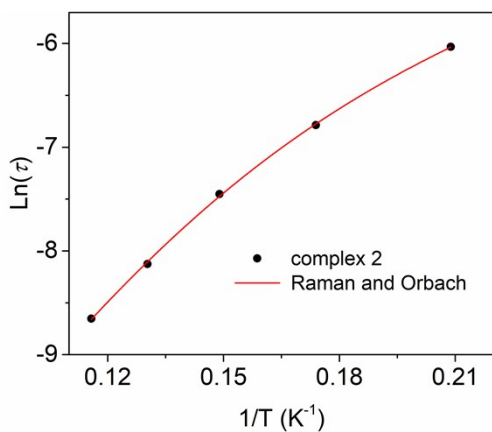


**Fig. S13** Plots of  $\ln(\tau)$  curves of  $1/T$  at applying dc field for **2**.

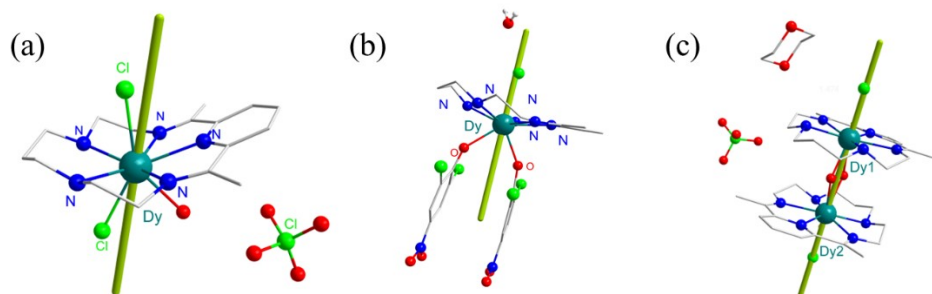


**Fig. S14** Orientations of the anisotropy axes for  $\text{Dy}^{3+}$  ions in **1** (a), **2** (b) and **3** (c) as calculated by MAGELLAN.